

Polarization stability and dynamics in a model for a polarization-isotropic laser that goes beyond third-order Lamb theory

N. B. Abraham,^{1,*} M. D. Matlin,^{1,2,†} and R. S. Gjøggia^{3,‡}

¹*Department of Physics, Bryn Mawr College, 101 North Merion Avenue, Bryn Mawr, Pennsylvania 19010-2899*

²*Department of Chemistry and Physics, Rowan College of New Jersey, Glassboro, New Jersey 08028*

³*Department of Physics, Widener University, Chester, Pennsylvania 19013*

(Received 13 March 1995; revised manuscript received 1 December 1995)

Instabilities and dynamical pulsations are common features of solutions of a model that includes the material variable dynamics for a laser with a polarization isotropic resonator and with a homogeneously broadened $j=1 \rightarrow j=0$ transition. These resemble in some respects features found in third-order Lamb theories under anisotropic conditions, such as splitting of the optical field into two relatively independent orthogonally polarized modes with different optical frequencies. At higher intensities the amplitudes and frequencies of these modes exhibit such strong coupling that a “two-mode” description loses its usefulness or effectiveness. Various periodic attractors with strong intensity and polarization pulsations are found for moderate excitation levels. Some of these attractors preserve the breaking of the polarization isotropy on average just as does any linearly polarized solution. But in some cases the dynamics restore the polarization isotropy on average. We also find other dynamical phenomena, including periodic and apparently chaotic states, often involving rapid switching between long interludes of nearly constant polarization, and homoclinic behavior.

PACS number(s): 42.60.Mi, 42.65.Sf, 42.55.Lt

I. INTRODUCTION

When a laser does not contain elements that constrain the electric field to a particular state of polarization, the vector nature of the amplitude of the electromagnetic field enters into the dynamics. If the material variables also enter the dynamics, then the vector nature of the material dipole moments also becomes important. Even when there are inevitable slight anisotropies in the cavity losses or differences in the cavity frequencies for fields of different polarization states, the dynamical evolution of the vector character of the electric field can be quite complicated. The dynamically evolving laser emission is not restricted only to the steady polarization state for which the system has the greatest gain or the least loss.

For isotropic and nearly isotropic lasers, the degeneracy of the angular-momentum states of the medium and the sizes of the decay rates of the intersublevel coherences and the population differences relative to the decay rates of the populations and of the electric-dipole moments play important roles in the selection of the polarization state of the field emitted by the laser. They contribute to a nonlinear (saturation induced) preference of the medium for stable emission with linear or circular polarization. This material preference can compete with or complement the preferences of the cav-

ity anisotropies in determining the final state or dynamical behavior.

This problem has been variously known as “a laser with a nearly isotropic resonator” [1–3], “the Zeeman laser” [4–7], and “a two-mode laser” [8], terms that as much as anything else indicate a conceptual framework for interpretation of the results or for the formulation underlying the theoretical approach and/or the intended application of the work.

The vector electric-field amplitude can always be represented by two scalar amplitudes of orthogonally polarized basis vectors, and several different decompositions are possible. But beyond the mathematical validity of such separations, many treatments give greater physical significance to them, concluding that the laser dynamics involves the interaction of two nearly degenerate modes that have the same longitudinal and transverse spatial patterns but differ in polarization state, frequency, and amplitude. The evolution of these modes has most often been described by two coupled equations for the complex modal amplitudes (typically using third-order Lamb theory), with cross saturation coefficients depending on Doppler broadening of the medium, detunings, and assumptions about the angular-momentum states of the medium and various decay rates; see, for example, [1,2,4–11].

A well-known, but often ignored, limitation of third-order Lamb theories, despite the considerable success of these models, is that accuracies of 10% or better in predicting the steady-state properties are possible only for excitations less than 20% above the lasing threshold [12]. Relaxing this limitation is one motivation of our present study as we examine polarization dynamics phenomena. A further limitation of both third-order Lamb theories and less approximate models limited to amplitude equations more generally is that the dynamical evolution of the atomic variables is neglected. In almost all previous studies, the dynamics of the atomic vari-

*Electronic address: nabraham@brynmawr.edu

†Electronic address: mmatlin@brynmawr.edu

‡Electronic address: pfbob@cyber.widener.edu

§Also at Institut Nonlinéaire de Nice, UMR 129, CNRS, Université de Nice-Sophia Antipolis, 1361 Route des Lucioles, F-06560 Valbonne, France. Electronic address: nabraham@doublon.unice.fr; Dipartimento di Fisica, Università degli Studi di Pisa, Piazza Torricelli 2, 50126 Pisa, Italy; and Departament de Fisica, Universitat de les Illes Balears, E-07071 Palma de Mallorca, Balears, Spain.

ables is adiabatically eliminated under the assumption that their decay rates are much larger than the field evolution rate, an assumption not fully applicable to many lasers. Indeed, for many atomic gas lasers, far-infrared molecular gas lasers, solid-state lasers, and low-pressure mid-infrared molecular gas lasers, the decay rate of the population variables is similar to or smaller than the cavity decay rate, making descriptions of the dynamics based on adiabatic elimination valid only very close to the lasing threshold.

Work including material variable dynamics has been relatively limited. Bakaev *et al.* [8] modeled dynamics in CO₂ lasers by adiabatically eliminating the atomic dipole moments but retaining variables for amplitudes of a spatial Fourier expansion for the population inversion(s) appropriate to a standing-wave laser. Puccioni *et al.* [13] included equations for dynamics of sublevel populations, atomic dipole moments, and quadrupole coherences between sublevels for incoherently pumped lasers, as, more recently, Vilaseca and co-workers [14] did for optically pumped far-infrared lasers. Others had earlier derived the appropriate formulas for the dynamical evolution of these variables (see, for example, [2,4,5,9,11,15] for incoherently pumped lasers), but they used these formulas only to assess the coefficients in a reduced (third-order Lamb) model for the coupled field amplitudes.

Since the work of Puccioni *et al.* [13] the importance of the material variables to the polarization dynamics has received a certain amount of renewed theoretical [14,16,17] and experimental [18,19] interest. Puccioni *et al.* found that when the laser cavity frequency was resonant with the material transition frequency there could be a polarization state instability of linearly polarized solutions for relatively low values of the excitation (near the lasing threshold). This instability occurs in the subspace of real variables, in which one could focus consideration on the amplitudes (rather than phases) of the complex variables.

We extend their studies to the time-dependent dynamics in the full model, where the phases are necessary if one is to find behavior that involves modes of two different frequencies. This common form of experimentally observed behavior is usually attributed to birefringence (phase anisotropies), but we find that it also exists in their model with isotropic parameters above the threshold for the ‘‘amplitude’’ instability.

The common explanations of nonsinusoidal pulsations in a polarized component and in the total intensity have been given in terms of two coupled amplitude equations with different cavity frequencies for the two modes (giving an Adler-type equation well known for nonlinearly coupled oscillators). But since we demonstrate here that similar phenomena arise when the material dynamics are included in the model for an isotropic laser, it remains an open question as to whether nonsinusoidal pulsations and total intensity pulsations are best explained by material variable dynamics (the option explored here) or by coupled amplitude equations with phase anisotropies. By studying both isotropic and anisotropic models that include material variable dynamics (without excluding or limiting the behavior *a priori* to only coupled amplitude equations) we believe we can gain the best possible understanding of the situation.

In the present work, we investigate the predictions of the

model for lasers tuned to resonance and with isotropic parameters. By keeping the dynamics of all of the material variables, we uncover a richer phenomenology of periodic pulsation phenomena, even lower instability thresholds than those found by Puccioni *et al.*, spontaneous selection of polarized eigenstates in the isotropic case, and dynamically induced frequency splitting of the optical spectrum into orthogonally polarized parts.

In another paper [17] we explored the polarization switching phenomenon that occurs with cavity detuning for either circularly or linearly polarized eigenstates (depending on residual anisotropies) and we compared those results with experimental phenomena observed in noble-gas lasers. A more complete generalization of earlier considerations of various atomic decay rates in the context of equations similar to those of Puccioni *et al.* has recently been worked out [16] in parallel with the present work.

The remainder of this paper is organized as follows. The model is presented in Sec. II, and the circularly and linearly polarized steady states and their stability analysis are presented in Sec. III. Numerical solutions for time-dependent behavior are presented in Sec. IV, while Sec. V is devoted to a summary and concluding remarks.

II. MODEL

The equations for the model are developed following the derivation in [13] for a field decomposed into components that are right and left circularly polarized interacting with a collection of atoms with a $j=1$ upper level and $j=0$ lower level. Analyses of the most general form of this kind of model with anisotropic parameters are presented elsewhere [16,17]. For simplicity of comparison with [13], we retain their assumptions and their notation for the particular case of isotropic conditions and resonance between the cavity and material transition frequencies:

$$dE_R/dt = -\kappa E_R + \kappa P_R, \quad (1a)$$

$$dE_L/dt = -\kappa E_L + \kappa P_L, \quad (1b)$$

$$dP_R/dt = -\gamma_{\perp} P_R + \gamma_{\perp} E_R D_R + \gamma_{\perp} E_L C, \quad (1c)$$

$$dP_L/dt = -\gamma_{\perp} P_L + \gamma_{\perp} E_L D_L + \gamma_{\perp} E_R C^*, \quad (1d)$$

$$dC/dt = -\gamma_c C - (\gamma_{\parallel}/4)[E_L^* P_R + E_R P_L^*], \quad (1e)$$

$$dD_R/dt = -\gamma_{\parallel}(D_R - \sigma) - (\gamma_{\parallel}/2)[E_R^* P_R + E_R P_R^* + \frac{1}{2}(E_L^* P_L + E_L P_L^*)], \quad (1f)$$

$$dD_L/dt = -\gamma_{\parallel}(D_L - \sigma) - (\gamma_{\parallel}/2)[E_L^* P_L + E_L P_L^* + \frac{1}{2}(E_R^* P_R + E_R P_R^*)]. \quad (1g)$$

Here E_R and E_L are the slowly varying amplitudes of right and left circularly polarized components of the fields, with κ the cavity loss; P_R and P_L are the associated slowly varying and suitably rescaled amplitudes of the dipole moment densities interacting with those fields, with γ_{\perp} their decay rate; D_R and D_L are the associated population inversion densities, γ_{\parallel} is the decay rate of the population inversions, and $\gamma_{\parallel}\sigma$ is

the excitation rate; C represents the quadrupole coherence between the $m=1$ and -1 sublevels of the upper level with γ_c its decay rate. We assume that the reference carrier wave for the dipole moments and fields is resonant with the atomic transitions. In the analysis that follows we take a renormalized time $\tau = \gamma_{\perp}^{-1} t$ and henceforth use the notation κ , γ_{\parallel} , γ_c to denote the losses and interlevel decay and mixing rates in proportion to γ_{\perp} .

Following the approach taken by Puccioni *et al.* and general considerations [11,16], we assume that the effect of collisional broadening on the transition is to give unequal values to γ_{\perp} , γ_c , and γ_{\parallel} . We fix the ratio of γ_{\parallel} to γ_{\perp} at 0.01, a reasonable order of magnitude for pressure broadened atomic gas lasers. Given the relaxation mechanisms at work in gas laser media, we further assume that realistic values of γ_c may range between γ_{\parallel} and γ_{\perp} . Indeed, we discover that the polarization state dynamics depend critically on the value of this parameter, and one might even use the comparison of numerical and experimental results to invert the model and determine an effective value of γ_c .

As detailed most clearly in the review by Lenstra [11] and elsewhere [20,21], the effect of isotropic collisions on the $j=1$ level permits separate relaxation rates for each of the tensorial components of this subpart of the atomic density matrix, which includes a scalar (the total sublevel population), a vector (including the difference in the sublevel populations), and a quadrupole (including the sublevel coherence C). The easiest way to incorporate the equilibration of the sublevel populations is to rewrite the final two equations as a sum and difference, with γ_{\parallel} as the decay rate of the sum and a separate (larger) decay rate γ_J for the difference in the populations, as discussed in [16]. However, to limit the wide parameter range for our present studies, we take all the population decay rates to be equal so that generally the system has a preference (from the character of the material saturation processes) for linearly polarized emission, with a strength that depends on the magnitude of the parameter ratio $\gamma_c/\gamma_{\parallel}$.

III. LINEARLY POLARIZED AND CIRCULARLY POLARIZED STEADY STATES AND THEIR STABILITY ANALYSIS

A. Steady-state solutions

For an isotropic cavity in resonance, Puccioni *et al.* [13] provide most of the needed information on the different steady-state solutions of the problem. These are summarized here.

(i) The off state

$$C = E_R = E_L = P_R = P_L = 0, \quad D_R = D_L = \sigma. \quad (2)$$

(ii) The circularly polarized states are (a) right circular

$$E_R = P_R = (\sigma - 1)^{1/2}, \quad E_L = P_L = C = 0, \quad D_R = 1, \\ D_L = (\sigma + 1)/2 \quad (3)$$

and (b) left circular

$$E_L = P_L = (\sigma - 1)^{1/2}, \quad E_R = P_R = C = 0, \quad D_L = 1, \\ D_R = (\sigma + 1)/2. \quad (4)$$

In these cases the total output intensity I ($\equiv |E_R|^2 + |E_L|^2$) is $\sigma - 1$. If $\gamma_J \neq \gamma_{\parallel}$ then $I = 4\gamma_J(\sigma - 1)/(3\gamma_J + \gamma_{\parallel})$, with corresponding changes in the values of D_L and D_R .

(iii) The linearly polarized states

TABLE I. Critical pump values for additional zero eigenvalues for stability of linearly polarized steady-state solutions. Note that all linearly polarized solutions have two zero stability eigenvalues corresponding to the global phase of the complex amplitude and the orientation of the electric-field vector (relative phase of the complex amplitudes of the left and right circularly polarized components).

γ_c	Phase instability threshold σ_p	Amplitude instability threshold σ_a
0.01	1.060 6	1.060 6
0.011	1.071 7	1.065 17
0.015	1.125 63	1.083 48
0.02	1.214 29	1.106 42
0.03	1.463 9	1.152 5
0.05	2.263 16	1.245 78
0.07	3.483 87	1.340 3
0.1	6.166 67	1.484 58
0.3	59.5	2.530 8
0.7	739.5	5.181 2
1.0	∞	8.01

$$|E_R| = |E_L| = |P_R| = |P_L| = \{2\gamma_c(\sigma - 1)/(3\gamma_c + \gamma_{\parallel})\}^{1/2}, \\ D_R = D_L = 1 + \{\gamma_{\parallel}(\sigma - 1)/(3\gamma_c + \gamma_{\parallel})\}, \quad (5) \\ |C| = \gamma_{\parallel}(\sigma - 1)/(3\gamma_c + \gamma_{\parallel}).$$

This result is not affected by the value of γ_J since the populations are equal. In these cases the total output intensity I is $4\gamma_c(\sigma - 1)/(3\gamma_c + \gamma_{\parallel})$, while the phase shift between E_R and E_L (and the consequent phase shifts between P_R and P_L and for C) determines the particular linear polarization. There is an infinity of solutions of this type with the relative phase between E_R and E_L varying between 0 and 2π .

Note that when $\gamma_c = \gamma_{\parallel}$ the total output intensity for this state is the same as for the circularly polarized states above. However as $\gamma_c \rightarrow 0$, the intensity of the linearly polarized solution goes to 0, while as $\gamma_c \rightarrow \infty$ the intensity rises to $4(\sigma - 1)/3$. Thus the linearly polarized state is more intense for $\gamma_c > \gamma_{\parallel}$ while the circularly polarized state is more intense for $\gamma_c < \gamma_{\parallel}$.

B. Stability analysis

1. Circularly polarized states

For the circularly polarized states, it is natural to imagine that since the population inversion of one transition is partly unutilized, the corresponding gain remains more than the loss. If this is true, the gain will quickly amplify any perturbation that excites the orthogonal circularly polarized component. Hence it is reasonable to expect, as observed by Puccioni *et al.* [13], that these states are unstable with respect to the growth of the other state when they exist (above threshold) and this instability causes a change of the circularly polarized initial state towards elliptical polarization, perhaps ending as linearly polarized behavior if that state is stable.

To verify this result and to compare our results with the work of others, we consider the linear stability of the solution with right circularly polarized emission. The equations that critically govern its stability are those for the left circularly polarized field, the left circularly polarized atomic dipole moment, and the quadrupole coherence. (The active

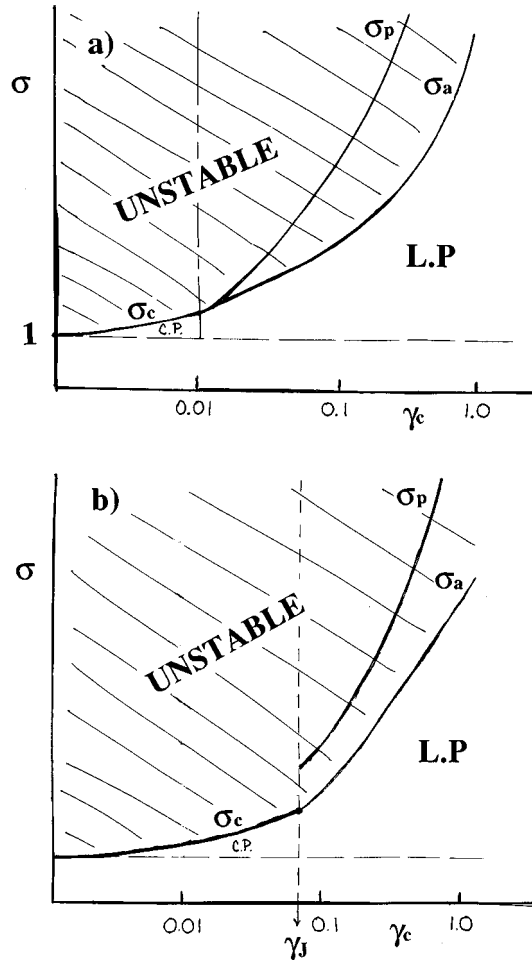


FIG. 1. Schematics of the stability diagrams for linearly and circularly polarized steady-state solutions in the phase space of pumping parameter σ versus the decay rate of the coherence γ_c for fixed values of the other parameters: (a) $\gamma_{\parallel}/\gamma_{\perp}=0.01$, $\kappa/\gamma_{\perp}=0.5$, $\gamma_J=\gamma_{\parallel}$; (b) $\gamma_J>\gamma_{\parallel}$. LP and CP indicate regions of stable linearly polarized and circularly polarized steady-state solutions, respectively.

field, polarization, and population inversion have the usual stability of a single-mode laser with a scalar amplitude in a Maxwell-Bloch equation model and the steady state is stable in this subspace so long as $\kappa<1+\gamma_{\parallel}$. In addition, the left circularly polarized inversion is stable.) The remaining six linearized equations separate into two sets of three equations for the variables E_L , P_L , and C^* and their complex conjugates, respectively. The result is a domain of stability for the circularly polarized states only in the condition of $\gamma_{\parallel}>\gamma_c$. This domain is bounded by the laser threshold from below and by a double Hopf bifurcation from above. The instability via the Hopf bifurcation is found above a critical value of σ , σ_c , given by

$$\sigma_c = 1 + 4\gamma_c(\kappa+1)(1+\kappa+\gamma_c)/[2\kappa^2+2\kappa + \gamma_{\parallel}(\kappa-1-\gamma_c)]. \quad (6)$$

The Hopf bifurcation frequency is given by

$$\Omega^2 = 2\gamma_c\kappa(\kappa+1)(\gamma_{\parallel}-\gamma_c)/\{2\kappa^2+2\kappa+\gamma_{\parallel}(\kappa-1-\gamma_c)\}. \quad (7)$$

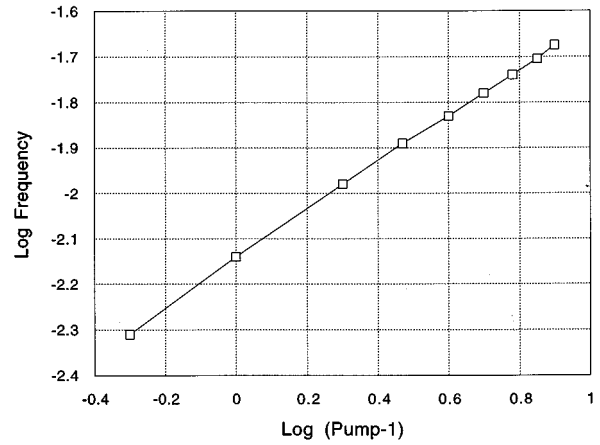


FIG. 2. Pulsation frequency of linearly polarized components of the time-dependent emission versus pump σ for $\gamma_c=0.01$, for which the total intensity remained constant.

In the domain of stability we have a situation that contradicts the naive expectation. We have inversion that provides amplification that exceeds the cavity losses on the transition that is suppressed, but the stability of the operating single polarized state indicates that there is absorption of any perturbation of that field. The more slowly decaying coherence term provides a contribution to the overall dipole moment, contributing absorption on the ‘‘off’’ transition as discussed in [16].

The eigenvectors for the instability indicate that it represents the onset of the off circularly polarized field with $\cos\Omega t$ modulation of its electric field (or with equally strong optical sidebands shifted by $\pm\Omega$ from the steady-state field of the other circularly polarized component which is resonant with the atomic frequency). The resulting initial modulations of the intensity of the off field and of the total intensity will be at frequency 2Ω . However, as shown in our numerical solutions, the final state that develops from this instability involves equal spectral power of the two circularly polarized components with symmetric detunings from the atomic resonance frequency.

For the parameter values we will use generally for our numerical solutions of Eqs. (1) ($\kappa=0.05$, $\gamma_{\parallel}=0.01$), the region of stable circularly polarized emission is relatively small in values of σ , existing approximately for $1.0<\sigma<1.06$. The instability arises via a Hopf bifurcation and its frequency goes to zero as γ_c approaches γ_{\parallel} .

While there is no physical reason to justify setting $\gamma_{\parallel}>\gamma_c$, since the decays of the amplitudes of the states due to spontaneous emission necessarily lead to decays of the coherences into which these amplitudes may enter, this choice provides a parameter region for the model in which the circularly polarized states are stable near threshold. This is of particular interest since a preference for circularly polarized emission has been noted experimentally for certain HeNe laser transitions, such as the $j=1\rightarrow j=0$ 1.523- μm line [4,9]. As shown elsewhere [16], if one includes in this model a decay rate for the population difference γ_J that is larger than γ_{\parallel} , then the circularly polarized state is stable for $\gamma_c<\gamma_J$, giving a physically reasonable and accessible region

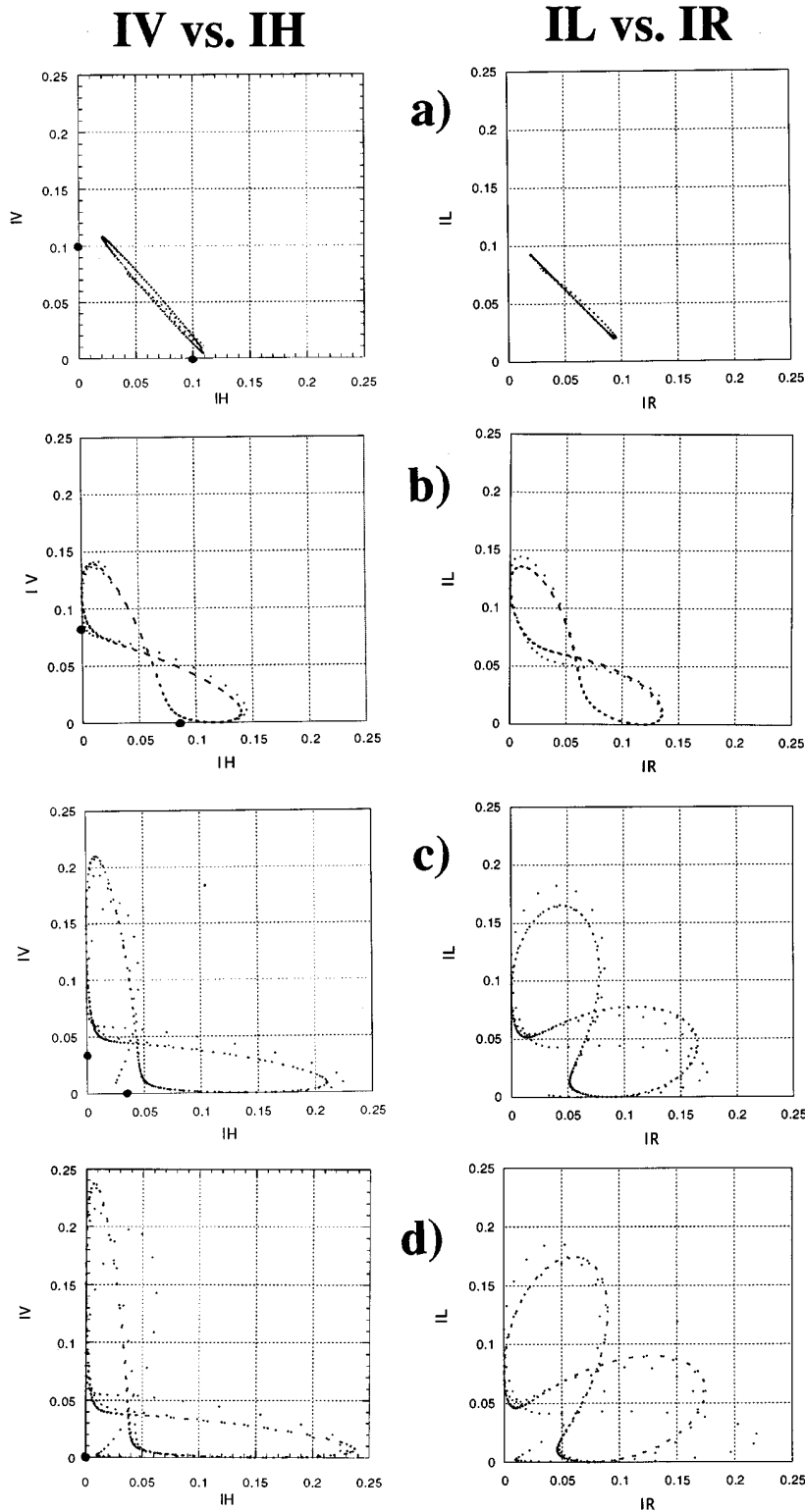


FIG. 3. Partial phase-space representations of time-dependent solutions with plots of the intensity of the vertically polarized component (IV) versus the intensity of the horizontally polarized component (IH) and the intensity of the left circularly polarized component (IL) versus the intensity of the right circularly polarized component (IR) for $\sigma=1.1$ and $\gamma_c=0.01$ (a), 0.005 (b), 0.001 (c), and 0.00 (d). Cases (b) and (c) represent combinations of parameters for which the nearest stable steady state (at lower pump values) is circularly polarized. The solutions shown here turn out to be long-lived transients, while the ultimate asymptotically stable solutions involve two frequency-split circularly polarized modes with constant intensities (see the text). Case (d) is one for which the instability threshold occurs at the lasing threshold $\sigma=1.0$. Here $\gamma_J=\gamma_{\parallel}=0.01$. Errant points indicate fast transients before the trajectory settled onto the long-lived but slightly unstable attracting subset. Selected points spaced equally in time (approximately 10–20 points per period) for approximately 50 periods are used to construct each figure. The dashed nature of some curves is an artifact of the sampling frequency for the plotted points being nearly a harmonic of the intensity pulsation frequency. Two of the family of linearly polarized steady-state solutions are indicated on the axes by solid circles.

defined by $\gamma_{\parallel} < \gamma_c < \gamma_J$ that has similar phenomenology. It is not easy to compare the results for different models in a simple way, but from the point of view of the third-order Lamb theory cross saturation rates, the range we propose for $\gamma_c/\gamma_{\parallel}$ carries the ratio of the cross-saturation coefficients to the self-saturation coefficient from values favoring circular polarization to neutral coupling to values favoring linear polarization.

2. Linearly polarized states

For the polarization isotropic laser medium and laser cavity, the linearly polarized states form an infinite family of solutions with arbitrary orientation of the vector of linear polarization in the transverse plane. According to the analysis of Puccioni *et al.* [13], these states are unstable with respect to perturbations in the intensity difference of the circularly polarized fields that preserve the total intensity. Thus

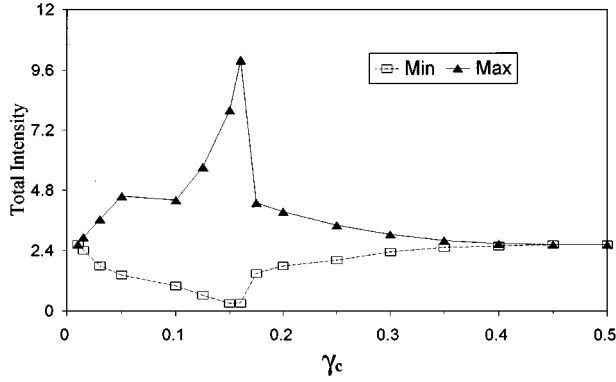


FIG. 4. Maximum and minimum values of the time-dependent solutions for the total intensity for different values of γ_c with $\sigma=3.0$.

these correspond to oscillations in the ellipticity of the emission. The linearly polarized steady states are also always unstable with a positive real eigenvalue when $\gamma_c < \gamma_{||}$ (or $\gamma_c < \gamma_J$, when $\gamma_{||} < \gamma_J$ [11,16]). When $\gamma_c > \gamma_{||}$, for our case, the instability occurs above a critical threshold value σ_a given by

$$\sigma_a = 1 + [(\kappa + 1)^2 + \gamma_{||}(\kappa + 1)](3\gamma_c + \gamma_{||}) / [2\kappa^2 + 2\kappa + \gamma_c(\kappa - \gamma_{||} - 1)], \quad (8)$$

which is more accessible than the usual single-mode laser second threshold (in that it exists for $\kappa < 1$ and generally for a lower value of σ), and with our parameters of $\kappa=0.5$ and $\gamma_{||}=0.01$ this can be written (for $\gamma_c < 1$) as

$$\sigma_a \approx 1 + 2.265(3\gamma_c + 0.01) / [1.5 - 0.51\gamma_c]. \quad (9)$$

The frequency of the 100% amplitude modulation of the orthogonally polarized (weak) field in the vicinity of this instability threshold is given by the expression

$$\Omega^2 = [2\kappa\gamma_{||}(\sigma_a - 1)](\gamma_c - \gamma_{||}) / [(3\gamma_c + \gamma_{||})(\kappa + \gamma_{||} + 1)], \quad (10)$$

which has the basic structure of the relaxation oscillation frequency of a single-mode class-B laser (the leading term in brackets), but multiplied by a factor $(\gamma_c - \gamma_{||})$, which may reduce this frequency to nearly zero. In the limit of large homogeneous broadening and $\gamma_c \gg \gamma_{||}$ we see that this frequency differs from the usual single-mode relaxation oscillation frequency by $(\frac{1}{3})^{1/2}$. As a modulation of the ellipticity of the solution, this instability causes, to higher order in the perturbation, a corresponding intensity modulation at twice this frequency. In fact, both the intensities of the strong and weak linearly polarized components oscillate at twice this frequency as well.

As we have noted in the discussion of the potential phenomena contained in the full 12 equations of the model, there is also the possibility of phase instabilities that would correspond to phase modulations that might lead to either rotation of the linear polarization or modulation of the ellipticity. Phase instabilities might also lead to frequency splitting (several frequencies in the optical spectrum) or to the onset of a solution involving two differently (orthogonally) polarized states with different optical frequencies. There are five

additional dimensions for this phase space. But there are really only four more dimensions available to the dynamics as the absolute (sum) phase of the system retains the neutral stability that is well known for autonomous optical systems. (It is the noise-induced diffusion of this total phase that leads to the linewidth of a traditional laser when projected as a diffusion of the phase of the electric-field amplitude.)

The four remaining phase variables have one negative eigenvalue that corresponds to the difference between the field and dipole phases. The eigenvalues for the angle of orientation (“the orientational phase”) of the linearly polarized electric-field vector (given by the relative phase between the circularly polarized components), the relative phase between the right and left circularly polarized dipole moments, and the phase of the quadrupole coherence are given by

$$\lambda^3 + \lambda^2(\kappa + \gamma_c + 1) + \lambda[\gamma_c\kappa + \gamma_c + \gamma_{||}(-\kappa/\gamma_c + \frac{1}{2})I/2] = 0. \quad (11)$$

Evidently there is a second zero eigenvalue (in addition to that associated with the sum of the phases), which corresponds to the neutral stability of the orientation of the linearly polarized state, and finally there may be yet a third zero eigenvalue (steady bifurcation) when

$$I = 4\gamma_c^2(\kappa + 1) / \gamma_{||}(2\kappa - \gamma_c), \quad (12)$$

which can be written in terms of a pumping threshold, using the expression for I in terms of the pump σ , as

$$\sigma_p = 1 + \gamma_c(\kappa + 1)(3\gamma_c + \gamma_{||}) / \gamma_{||}(2\kappa - \gamma_c), \quad (13)$$

subject to the condition $2\kappa > \gamma_c$. Note that there is an asymptote at which this instability threshold reaches infinity for $2\kappa = \gamma_c$. For example, for $\kappa=0.5$ and $\gamma_{||}=0.01$ we have $\sigma_p > 1 + 150\gamma_c(3\gamma_c + 0.01) / (1 - \gamma_c)$. The linearly polarized steady-state solutions are unstable for values of σ or I above these thresholds.

The neutral stability of the orientation of the linearly polarized solutions appears even though there is more population inversion than the normal threshold value for exponential growth of the suppressed field. Despite the excess inversion there is neither net gain nor loss [16]. The zero eigenvalue for the relative phase of the fields means that appropriate perturbations of the amplitude of the off linearly polarized field, the off dipole, or the imaginary part of the coherence C lead to a simple diffusive rotation of the linearly polarized state in real space.

Comparing these two thresholds we find that the “amplitude instability” (which modulates the ellipticity) always occurs at a lower value of the pump than the phase instability. For example, for $\kappa=0.5$ and $\gamma_{||}=0.01$ we have values as shown in Table I. The two thresholds are very close over a range of γ_c less than $2\gamma_{||}$, but for large values of γ_c approaching κ the phase instability threshold goes asymptotically to infinity.

Paralleling the result for the stability of the circularly polarized solutions [16], the introduction of a decay rate γ_J (for the difference of the R and L population differences) that is larger than $\gamma_{||}$ limits the domain of stability of the linearly

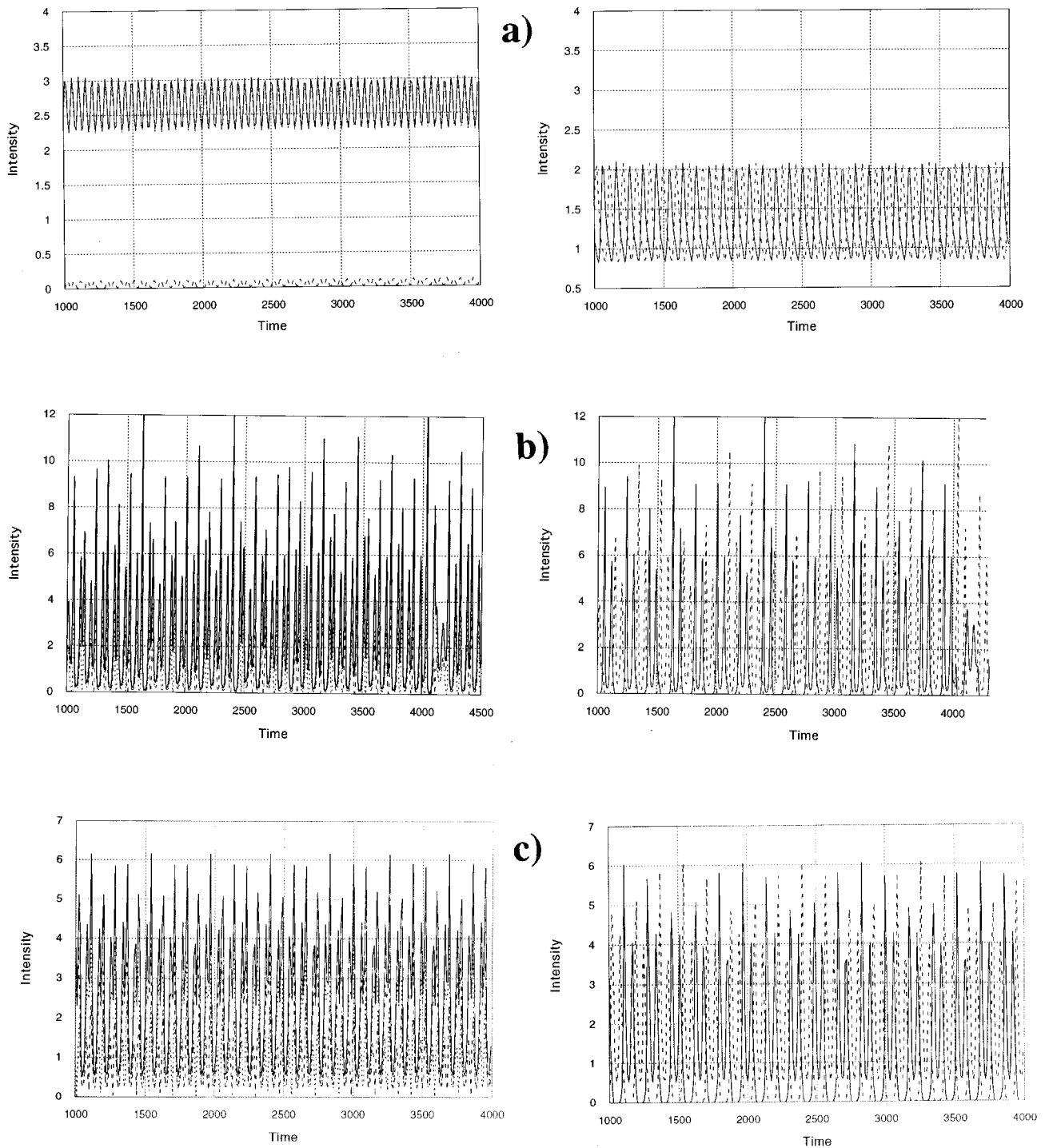


FIG. 5. Intensity time series for $\sigma=3.0$. Plots in the left-hand column give the total intensity (solid line), the intensity of vertically polarized component (dashed line), and the intensity of horizontally polarized component (dotted line). Plots in the right-hand column give IL (dashed line) and IR (dotted line). Time is in units of γ_{\perp}^{-1} . Values of γ_c are (a) 0.3, (b) 0.16, and (c) 0.13.

polarized solutions to $\gamma_c > \gamma_J$. This gives, within the model, a physically accessible region of circularly polarized emission $\gamma_{\parallel} < \gamma_c < \gamma_J$ appropriate to describe some lasers. This comes about from a shift in the boundary for the amplitude instabilities of the linearly polarized state, but there is no shift in the instability condition for the phase instabilities, so the collision of these boundaries for $(\gamma_c = \gamma_{\parallel} = \gamma_J)$ is lost when the collision takes place at $\gamma_c = \gamma_J$ with $\gamma_J > \gamma_{\parallel}$.

3. Summary of observations on the stability of these steady-state solutions

At the laser threshold, there is a bifurcation of two circularly polarized solutions and an infinite set of linearly polarized solutions. Just above the threshold for laser generation, the circularly polarized states are both stable (the system is bistable) when the output intensity for circularly polarized emission is greater than the output intensity for one of the

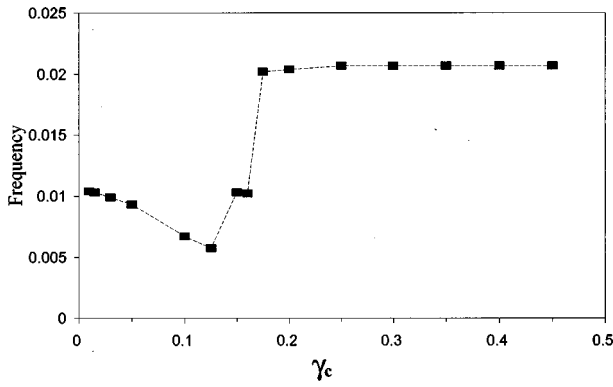


FIG. 6. Pulsation frequency of IV and IH vs γ_c for $\sigma=3.0$.

degenerate infinity of linearly polarized solutions (this requires $\gamma_c < \gamma_{||}$ when $\gamma_{||} = \gamma_J$, or $\gamma_c < \gamma_J$ more generally). When the linearly polarized output is greater than the circularly polarized output ($\gamma_c > \gamma_{||}$ when $\gamma_{||} = \gamma_J$, or $\gamma_c > \gamma_J$ more gen-

erally) the linearly polarized emission is stable (though with the possibility for diffusion of the orientation of the linear polarization). This choice of the preferred (stable) polarization basis is a form of the “maximum emission principle” [22].

Elliptically polarized solutions, of arbitrary ellipticity, exist at the neutral stability boundary $\gamma_c = \gamma_{||}$ (or $\gamma_c = \gamma_J$ more generally). We have numerical evidence that these solutions, if they exist off this boundary, are unstable.

The Hopf bifurcation–steady bifurcation collision that occurs when $\gamma_c = \gamma_J$ (which is heightened when $\gamma_{||} = \gamma_c = \gamma_J$, as then there are simultaneously three $\lambda=0$ eigenvalues [for the global phase, for the ellipticity, and for the orientation of the major axis of the polarization ellipse (azimuth)]) has a special feature. The frequency of the Hopf bifurcation goes asymptotically to zero at the collision, making this a generalized Takens-Bogdanov point [23] with interesting dynamics in the vicinity, as will be seen numerically. All of these results of stability analyses are summarized schematically in Fig. 1.

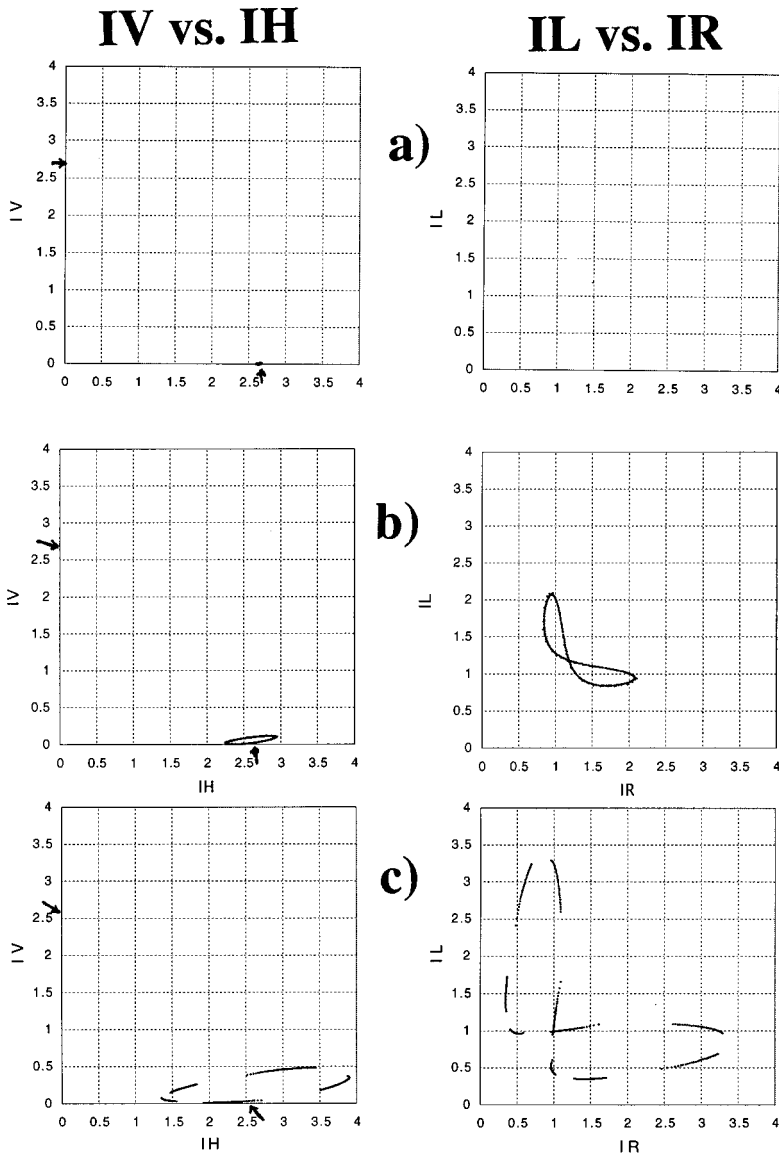


FIG. 7. Plots of IV vs IH and of IL vs IR for $\sigma=3.0$ as in Fig. 3 for $\gamma_c=0.5, 0.3, 0.17, 0.165, 0.16, 0.15, 0.13, 0.1, 0.03, 0.015, 0.01, 0.00$ for (a)–(l), respectively. Two of the family of linearly polarized solutions are indicated on the axes by arrows.

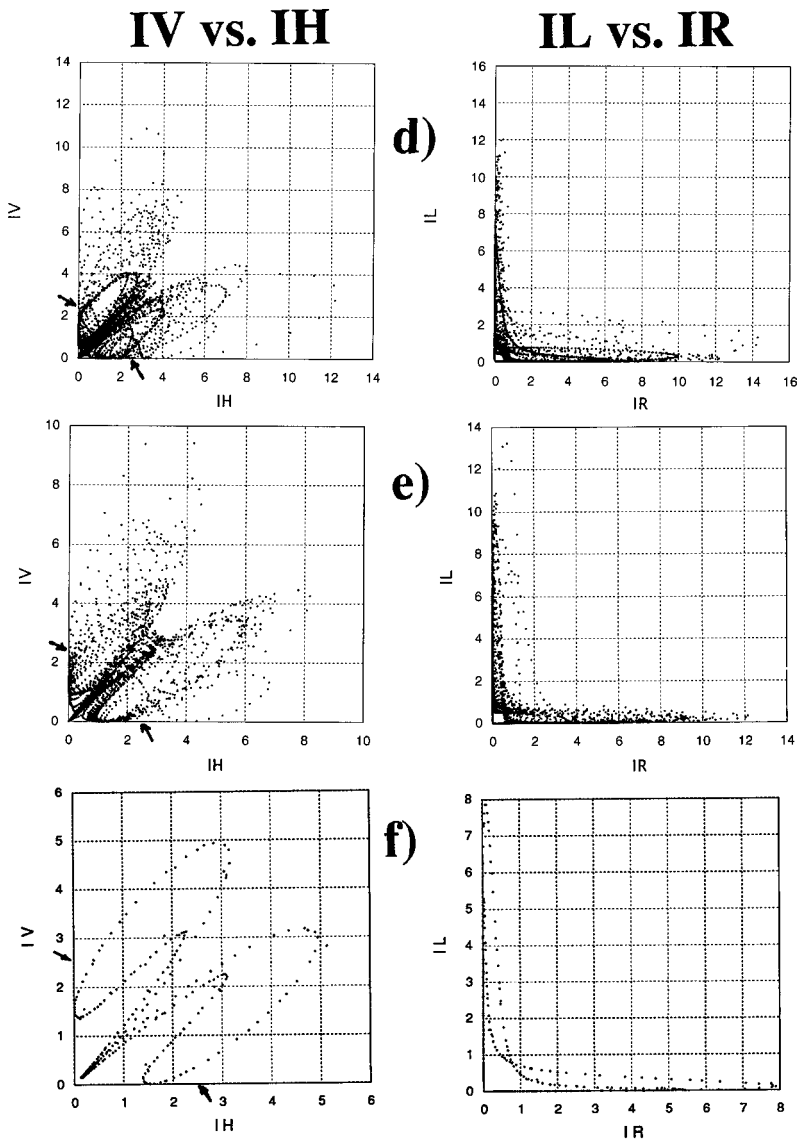


FIG. 7. (Continued).

IV. NUMERICAL RESULTS FOR TIME-DEPENDENT SOLUTIONS

A. Method of solution

For our numerical solutions the equations were solved with a fourth-order Runge-Kutta integration routine with a fixed time step taken to be small enough to give convergent solutions. For the studies reported here we will take $\kappa=0.5$ and $\gamma_{\parallel}=0.01$.

B. Results for the “neutral stability case”

For $\gamma_c = \gamma_{\parallel} = 0.01$, where both the ellipticity and the orientation of the major axis of the polarization state (as well as the global phase of the complex amplitude) are free to diffuse (have zero eigenvalues) even in the “stable” steady state, there is the amplitude instability threshold for time-dependent dynamical solutions at a pump value $\sigma=1.06$. The time-dependent solutions have a constant total intensity (over a wide range of pump parameters explored), though this value exceeds the common value of the intensity of any of the steady-state solutions. This corresponds to a further generalization of the maximum emission principle, as noted by

Casperson [22], who found greater average emission for time-dependent solutions than for steady states in a different laser system.

Here in a typical numerical result, the intensities of the linear and circularly polarized components of the field oscillate sinusoidally and out of phase with different percentage modulations, though those percentage modulations could be varied by perturbations or changes in the initial conditions. This is one of several indications that the dynamical laser operation has been established as a combination of two optical fields of orthogonal polarization states (which are typically elliptically polarized) with different optical frequencies. The constancy of the amplitudes of the selected polarization basis states is reflected in the sinusoidal (beat frequency) nature of the intensity pulsations of a different polarized component of the emission. The ellipticity of these chosen states depends sensitively on the initial conditions and any perturbations. The pulsation frequency in the unstable range of parameters is shown in Fig. 2, where it is plotted against the degree to which the pump parameter (σ) is above threshold for laser action. This clearly indicates that the pulsation frequency (which is the splitting between the two strongest

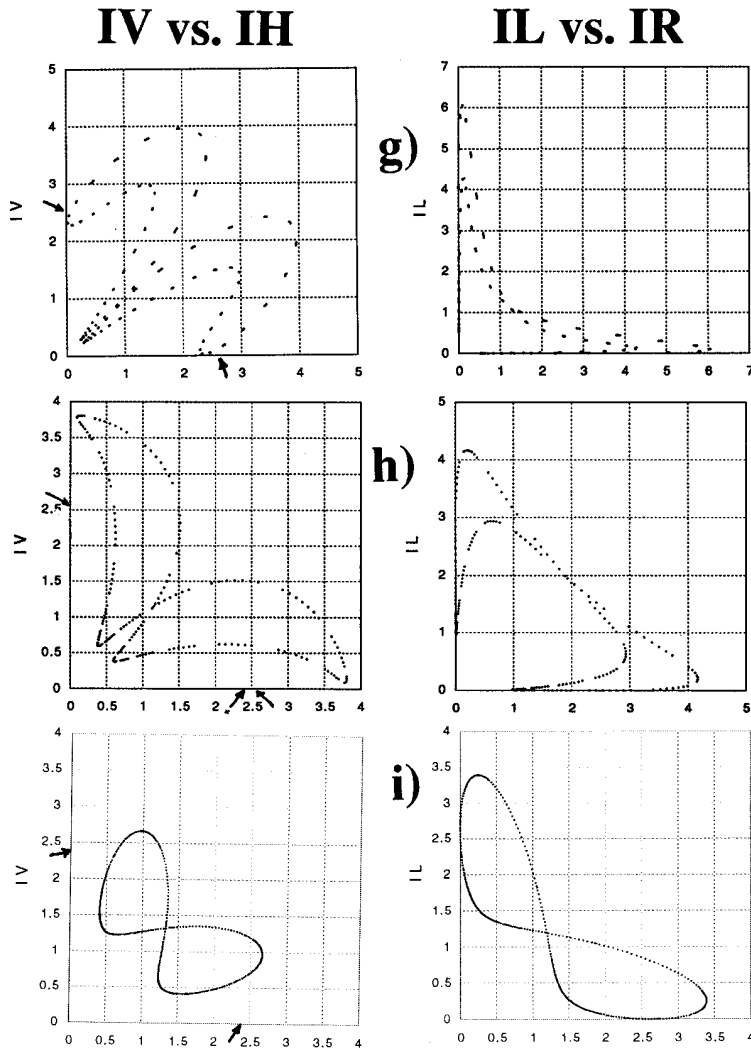


FIG. 7. (Continued).

components in the optical spectrum of the field) grows as the square root of the excess pump over threshold, just like a Rabi frequency or a relaxation oscillation frequency in a ‘‘class B’’ laser and just like the characteristic frequencies of the complex conjugate eigenvalues found in the stability analysis of Sec III B, even though for these parameters there are no complex conjugate eigenvalues at threshold. This splitting of the frequencies of the two modes is also reminiscent of the behavior of multimode dye lasers, which spontaneously select two modes (or narrow groups of modes) separated by a factor that grows proportionally to the square root of the excess pump over threshold [24–26].

C. Results for pumping near threshold

To better understand this behavior, we first study it in more detail as a function of γ_c and detuning near the lasing threshold (for $\sigma=1.1$). These cases should be readily comparable to solutions found for third-order Lamb theory, except that third-order Lamb theory does not allow for the amplitude instability for a polarization isotropic laser. For values of $\gamma_c \geq 0.02$, the output is stable linearly polarized behavior at the resonance frequency of the cavity and the material transition. Solutions with different orientations of their linear polarization are easily excited by shifts in the relative phase of the fields and polarizations and the corresponding shift of

the phase of C , as noted for steady states in Sec. III A. The orientation of the linearly polarized states can be perturbed arbitrarily by phase shifts in the fields, the dipoles, and the coherence C and continuous noise causes diffusive motion of the orientation of this linearly polarized state.

To explore the regions of parameter space others have observed to be unstable or time dependent, we note that when $\sigma=1.1$, the amplitude instability threshold has been crossed for values of $\gamma_c \leq 0.018$. To try to understand the dynamics through a partial representation in phase space, we show examples of the variation of the intensities of linearly polarized and circularly polarized components in plots for $\gamma_c \leq 0.02$ in Fig. 3. In this zone we see instabilities involving both the relative intensities of the two modes and a frequency splitting of the sort studied by Grossman and Yao [27].

For $\gamma_c < 0.01 = \gamma_{l1}$ we find long transients in the form of pulsations in both the total intensity and in the polarized intensities, with the system dwelling for relatively long times in each of the two circularly polarized unstable states (though with growing or decaying intensity) followed by a more rapid switching to the other circularly polarized state. The dwell time becomes longer as γ_c is reduced to zero. For such low values of γ_c the linearly polarized steady-state solutions have nearly disappeared in a collapse onto the un-

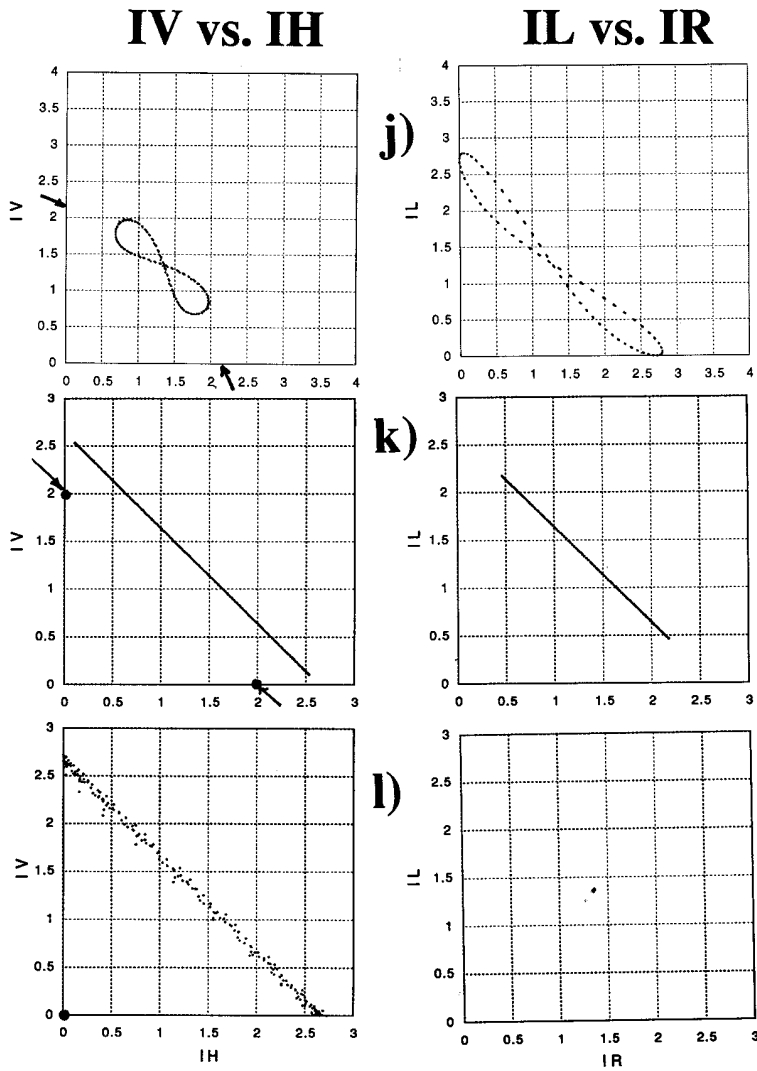


FIG. 7. (Continued).

stable off solution. Generally the trajectories evidently avoid the proximity of the unstable steady-state solutions (linearly or circularly polarized) that are indicated. However, after long evolution on the type of weakly unstable and characteristic attractors shown in Figs. 3(b)–3(d) the solutions settle onto two circularly polarized modes with symmetrically detuned optical frequencies. The resulting total intensity is constant, while the intensities of vertically and horizontally polarized components are 100% modulated at the beat frequency [28]. Because the splitting frequency is much smaller than the overall optical frequency, this is a state in which at each instant the emission is linearly polarized, but the orientation of the polarization vector rotates in time, just as would be expected from Zeeman splitting of the magnetic sublevels from an applied magnetic field. In this case the splitting is a spontaneous consequence of the dynamics [28].

D. Higher pump levels: Strong output fields

We next explore the behavior of the system in resonance for the pump parameter $\sigma=3.0$ where the steady-state solutions are almost always unstable except for γ_c larger than about 0.5. By raising γ_c above 0.01 ($=\gamma_0$), the total intensity begins to pulse. Figure 4 shows the upper and lower bounds of the total intensity pulsations versus γ_c . Figure 5 shows the

nature of the pulsations in the total intensity for several different characteristic regions and in the intensities of the linearly and circularly polarized components of the output, in time as well as in certain phase-space projections. Figure 6 gives the variation of the pulsing frequency of the linearly polarized components of the intensity versus γ_c . For $\gamma_c < \sim 0.15$, the total intensity pulses at twice the frequency of the pulsations of the intensities of linearly polarized components, while for $\gamma_c > \sim 0.17$ the total intensity has the same pulsation frequency as the intensities of the polarized components. For values of γ_c near 0.16, the intensity pulsations are quite large and rather more irregular. Figure 7 shows variations of the intensities of orthogonally polarized components of the emission for a wide range of values of γ_c .

There are four primary domains of behavior as a function of γ_c .

(i) For low γ_c (near and below 0.01) the behavior is similar to that found for $\gamma_c=0.01$ at $\sigma=1.1$ (see Fig. 3), that is, two orthogonal elliptically polarized solutions of different frequencies, which lead to out of phase pulsations of either pair of right and left circularly polarized (or vertically and horizontally polarized) intensities and no pulsations in the total intensity. Note that for $\gamma_c=0$, the two states are exactly circularly polarized (constant circularly polarized intensities,

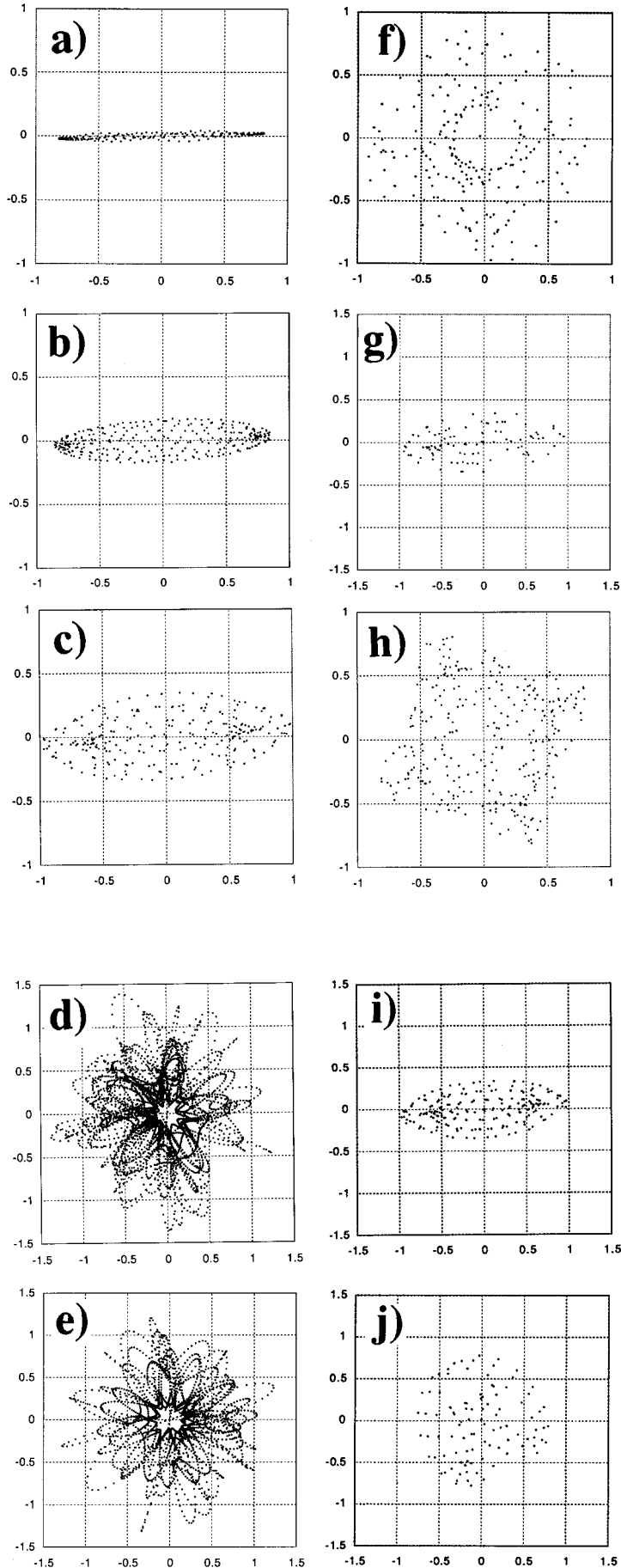


FIG. 8. Plots of the real electric-field vector $\text{Re}(E_y)$ vs $\text{Re}(E_x)$ with a carrier frequency of about $\frac{1}{50}$ for $\sigma=3.0$ and different values of γ_c [0.5, 0.3, 0.17, 0.165, 0.16, 0.15, 0.1, 0.03, 0.01, 0.0 for (a)–(j), respectively]. Polarization isotropy is evidently restored on average after sufficiently long times for the conditions of (d)–(h) and (j). [With the carrier frequency added, purely linearly polarized emission of constant amplitude would give a line through the origin as for (a), circularly polarized emission of constant amplitude would give a circle centered at the origin, and elliptically polarized emission of constant amplitude would give an ellipse centered at the origin. Points are taken as for other time series at 10–20 points per period of the intensity modulations for 40–50 periods.]

100% modulated linearly polarized intensities, constant total intensity) as found at $\sigma=1.1$ for $\gamma_c < 0.01$.

(ii) For γ_c between 0.015 and 0.15, there are pulsations in the total intensity with a dominant frequency that is twice the dominant frequency of the pulsations of the polarized intensities. The partial phase-space portraits of these periodic attractors are symmetric in the intensities of orthogonally polarized eigenstates.

It may be that the special dynamics in these first two regions arise from the strong phase dynamics (as well as the amplitude dynamics) that are induced by the instability of phase eigenvalues as well as the amplitude eigenvalues.

(iii) For γ_c between 0.17 and 0.4, the pulsations are in the vicinity of a linearly polarized steady-state solution with modulation of both the total intensity and the tip angle of the polarization state.

(iv) For γ_c higher than 0.4, the pulsations cease and the laser operates with a linearly polarized output at an intensity of about 2.66, as predicted for these steady-state solutions in this range of γ_c . These linearly polarized solutions are stable in this case, except for their neutral stability with regard to orientational diffusion.

The bifurcation from the stable horizontally polarized solution to the time-dependent solution as γ_c is decreased from the stable single-mode region represents (from numerical studies) the onset of a weak vertically polarized field at two symmetrically detuned optical frequencies (or, equivalently, at the resonant carrier frequency with 100% modulation of the amplitude). This instability initially does not lead to modulation of the total intensity (at least not to the same order of perturbation). Instead it represents a modulation of the ellipticity of the solution.

As the vertically polarized component grows stronger in amplitude for lower values of γ_c the once second-order disturbance of the total intensity becomes clearer as a modulation at twice the frequency of modulation of the vertically polarized amplitude. The total intensity, the horizontally polarized intensity, and the vertically polarized intensity all oscillate at twice the modulation frequency of the vertically polarized amplitude, as is evident in Fig. 5 for $\gamma_c=0.3$. In the 12-dimensional phase space this corresponds to the birth of a simple limit cycle of constant intensity that subsequently deforms, having two oscillations on the surface of a small torus for each revolution. From the point of view of the Poincaré sphere, the motion of the state vector is an oscillation alternately above and below the equatorial plane in a kind of figure-8 shaped trajectory.

Returning to the birth of this instability at $\gamma_c=0.4$, the vertically polarized intensity is nearly zero and the horizontally polarized intensity and the total intensity weakly pulse. Since the modulation is very weak here, we can see clearly the infinitesimal effects just above the bifurcation threshold. The strong horizontally polarized component operates on average with an optical frequency given by the cavity frequency (with a weak frequency and phase modulation), while the vertically polarized component operates at two optical frequencies that are detuned by about ± 0.01 .

As γ_c is reduced below 0.4 the operation remains predominantly linearly polarized, though the amplitude of the pulsations increases. For $\gamma_c=0.3$ the pulsations are about 10% of the horizontal intensity and the ratio of the two av-

erage intensities $\langle I_H \rangle / \langle I_V \rangle$ is about 25. For $\gamma_c=0.2$ the horizontal mode has about a 25% modulation and the ratio of the two average intensities is about 17.

In between the second and third regions of different behavior, near $\gamma_c=0.16$, we see a destabilization of the simple, asymmetric periodic oscillations found for higher γ_c 's. Here the trajectories pass near the point of zero total intensity. In the phase plots of IV vs IH in Fig. 7 we see evidence of two unstable nearly linearly polarized attractors, ellipses near the vertical and horizontal axes, which are "glued" together to form the more elaborate attractor. The total intensity pulsation frequency, which was equal to the pulsation frequencies of the linearly polarized components for larger values of γ_c , shifts to being double the frequency of the intensity pulsations of polarized components for lower values of γ_c . We see the abruptness of this transition in Fig. 6.

At $\gamma_c=0.165$ the apparently complex behavior seen in the plot of the linearly polarized intensities masks a periodic pulsation evident in the IL vs IR plots in Fig. 7 that repeats after every two pulses in the circularly polarized intensities. In this case the dynamics causes a rotation of the orientation of the linearly polarized states that does not necessarily give a rational ratio between the rotation rate and the pulsation rate. The trajectory spends long times alternately in left or right circularly polarized emission with changing intensity before switching to the other polarization state relatively rapidly. In the Poincaré sphere representation this involves long residency along the polar axis.

For $\gamma_c=0.16$ the sustained pulsations and phase portraits seem to indicate a truly chaotic behavior, as is evident in the scatter of points which do not settle onto an attracting subset in the plots of both linearly and circularly polarized intensities in Fig. 7(e). For lower values of $\gamma_c \sim 0.14-0.145$, where the trajectories approach the (0,0) unstable fixed point in a kind of homoclinic trajectory, the speed of the trajectory and the corresponding frequency of the orbits (see Fig. 6) slows to near zero, as expected.

In the third and fourth regions of behavior our attractors (linearly polarized or modulated solutions) are states that have broken the cylindrical symmetry of the equations. However, in the first two regions the cylindrical symmetry that was broken for the steady-state solutions is restored by the dynamics on average [29]. This restoration of the symmetry is indicated by the plots in Fig. 8 of the real electric-field vector in real space and of the orientational angle of this electric-field vector in time. A small carrier frequency has been selected so that circularly polarized behavior is not frozen in angle but rotates clockwise or counterclockwise depending on whether the solution is right or left circularly polarized. This carrier frequency causes constant amplitude solutions of circular polarization to trace out circles in real space (with a slope in the orientation angle versus time) and causes constant amplitude solutions of linear polarization to trace out lines through the origin at fixed orientation angles (with jumps of π rad in the orientational phase).

As a final note, we point out that the dynamical pulsations that have a particular linear polarization on average are susceptible to perturbations (or diffusion in the presence of noise) of the orientation of the major axis of their polarization ellipse. An illustration of this is given in Fig. 9, where only the initial conditions have been changed. Figure 9(a)

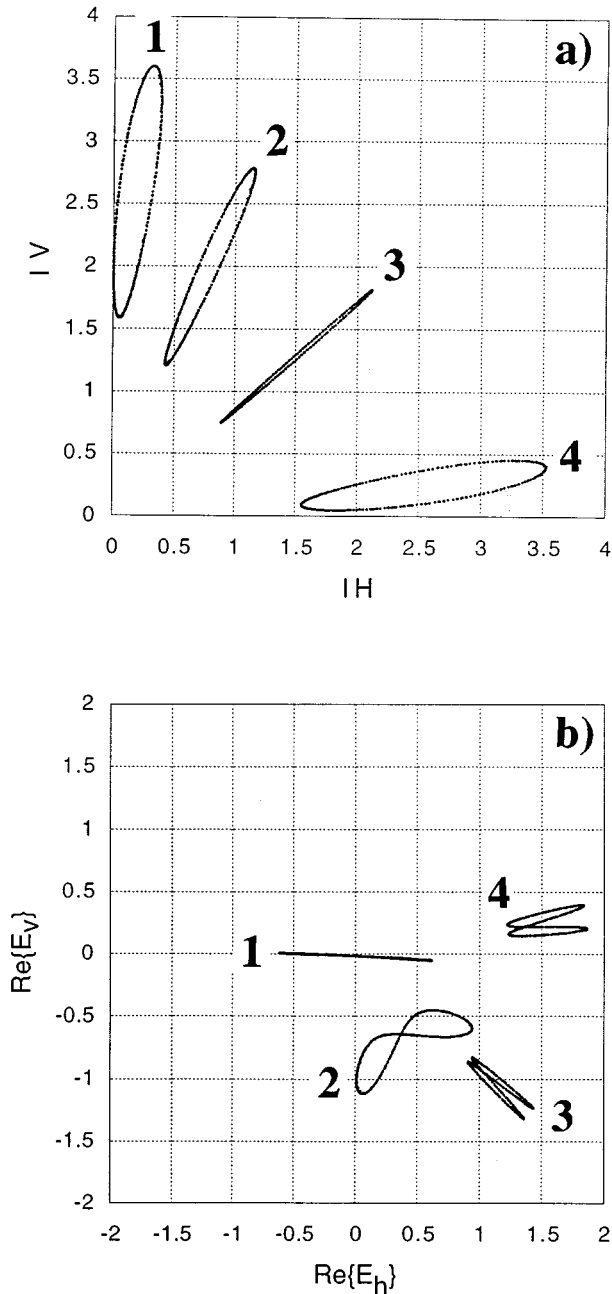


FIG. 9. (a) Plots of the intensity of the vertically polarized emission versus the intensity of the horizontally polarized emission for solutions with $\gamma_c=0.3$ and $\sigma=3.0$, but with different initial conditions. (b) Plots of the $\text{Re}\{E_V\}$ vs $\text{Re}\{E_H\}$ for the same solutions. These show how perturbations induce diffusion of the major axis orientation with respect to the center of (b) of the major axis of the average polarization state.

shows the intensities of the linearly polarized components, while Fig. 9(b) shows the evolution of the real part of the vector electric field. In each case the dynamics is essentially the same on the Poincaré sphere, but the projections are different. In the presence of continuous noise there would be diffusion among a whole family of these states.

V. SUMMARY

A critical feature of these results relative to the consideration of this model by Puccioni, Tratnik, Sipe, and Oppo [13]

is that we show that the fully developed time-dependent dynamics of their model contains not only amplitude modulations, as indicated by the primary bifurcation phenomenon that they reported, but also spontaneous splitting of the optical frequencies of the two modes and strong phase modulation as well. Already one might infer that, since 100% amplitude modulation of a field that is initially zero means the creation of two sidebands. Appreciating that the linearly polarized strong field has arbitrary orientation, one should not be surprised at a dynamical mixing of the strong resonant field and the orthogonally polarized sidebands to create two strong fields of nearly orthogonal polarization, both of which are detuned from resonance. Once the amplitude pulsations of both fields are strong, the likelihood is enhanced of frequency dynamics as the two fields compete for stronger gain on resonance.

We have demonstrated that even with perfect symmetry (isotropy) in the parameter space and perfect resonance between the cavity and the material frequencies, the dynamical coupling of the vector field and the medium can split the field into two modes with different polarization states and different frequencies (or give the strong mode two weak sidebands having the orthogonal polarization and different optical frequencies). Furthermore, the fully developed dynamics give dramatic amplitude and frequency modulations to the fields. These are features that do not appear in coupled amplitude (third-order Lamb theory) models without the addition of anisotropies.

We believe that this model, when considered in the expanded parameter space, provides an adequate structure of nonlinear interactions to extend the usual third-order Lamb theory to stronger fields and higher values of the pump. We believe it can be useful as the first step in considering models that can more completely model the polarization preferences and dynamics of lasers with nearly isotropic cavities. Adjustments in the parameters γ_c and γ_l permit consideration of lasers that have linearly polarized, circularly polarized, or arbitrarily polarized emission in the pump parameter range that gives time-independent solutions. In this way, one has an initial indication of possible behavior in lasers with other $j \rightarrow j'$ transitions, since, at the level of third-order Lamb approximations, this model can emulate different strengths of this material saturation preference for linearly or circularly polarized emission. The strengths of these self- and cross-saturation coefficients are specifically evaluated for near-threshold operation in [16]. Investigation of whether the predicted amplitude instabilities for these cases are in reasonable agreement with experiments, when appropriate values are taken for the different decay rates, will be a natural extension of the present work.

The results of stability analyses presented here are also a first step along the study of the response of such lasers to technical and intrinsic noise and of the subtleties of the laser linewidths, correlated noises, intensity fluctuations, and phase sensitive noise in the presence of material variable dynamics. Even below the threshold for dynamical instabilities these phenomena will be strongly affected by eigenvalues with small real parts. This should enliven and enlarge the considerations represented by the studies reported in [19] and their extensions [28].

ACKNOWLEDGMENTS

We are pleased to acknowledge helpful discussions with G. L. Lippi and G. L. Oppo on the theoretical modeling and are particularly grateful to the latter for sharing with us extensions of [13] prior to publication. Further discussions with E. Arimondo, M. Fleischhauer, J. M. Gambaudo, G. Huyet, G. Iooss, Ya. I. Khanin, L. Svirina, G. Mindlin, S. Rica, M. San Miguel, C. A. Schrama, J. R. Tredicce, and J. P. Woerdman have been stimulating and enlightening as we

have interpreted our results. We are also grateful to E. Roldán, G. J. de Valcárcel, and R. Vilaseca for helpful discussions and for their sharing their parallel work (especially [30]) on this problem prior to its publication. We are particularly grateful to C. A. Schrama and J. P. Woerdman for sharing their results of work in progress on this and related models [28], which gave us insight and guidance to correct some of our earlier work. R.S.G. acknowledges the support of NSF Grant No. ECS-8822990.

-
- [1] P. Paddon, E. Sjerne, A. D. May, M. Bourouis, and G. Stéphan, *J. Opt. Soc. Am. B* **9**, 574 (1992).
- [2] A. P. Voitovich, *J. Sov. Laser Res.* **8**, 555 (1987); A. P. Voitovich, L. P. Svirina, and V. N. Severikov, *Opt. Commun.* **80**, 435 (1991).
- [3] L. Svirina, *Opt. Commun.* **111**, 370 (1994).
- [4] R. L. Fork and M. Sargent III, *Phys. Rev.* **139**, A617 (1965); R. L. Fork, W. J. Tomlinson, and L. J. Heilos, *Appl. Phys. Lett.* **8**, 162 (1966); M. Sargent III, W. E. Lamb, Jr., and R. L. Fork, *Phys. Rev.* **164**, 436 (1967); **164**, 450 (1967); W. J. Tomlinson and R. L. Fork, *ibid.* **164**, 466 (1967); *Phys. Rev. Lett.* **20**, 647 (1968); *Appl. Opt.* **8**, 121 (1969); C. H. Wang, W. J. Tomlinson, and R. T. George, *Phys. Rev.* **181**, 125 (1969).
- [5] M. Sargent III, M. O. Scully, and W. E. Lamb, Jr., *Laser Physics* (Addison-Wesley, Reading, MA, 1974), Chap. 12 and Appendix F.
- [6] A. Le Floch and R. LeNaour, *Phys. Rev. A* **4**, 290 (1971).
- [7] A. D. May, E. Sjerne, P. Paddon, and G. Stéphan, *Phys. Rev. A* **53**, 2829 (1996).
- [8] N. G. Basov, M. A. Gubin, V. V. Nikitin, and E. D. Protsenko, *Kvant. Elektron.* **11**, 1084 (1984) [*Sov. J. Quantum Electron.* **14**, 731 (1984)]; S. A. Gonchukov, *Laser Phys.* **1**, 634 (1991); D. S. Bakaev, V. M. Ermachenko, V. Yu. Kurochkin, V. N. Petrovskii, E. D. Protsenko, A. N. Rurukin, and R. A. Shanin, *Kvant. Elektron. (Moscow)* **15**, 37 (1988) [*Sov. J. Quantum Electron.* **18**, 20 (1988)].
- [9] H. de Lang, *Philips Res. Rep.* **19**, 429 (1964); D. Polder and W. van Haeringen, *Phys. Lett.* **19**, 380 (1965); W. van Haeringen, *Phys. Rev.* **158**, 256 (1967); *Phys. Lett.* **24A**, 65 (1967); D. Polder and W. Van Haeringen, *ibid.* **25A**, 337 (1967); H. de Lang, *Philips Res. Rep. Suppl.* **8**, 1 (1967); *Physica* **33**, 163 (1967); W. van Haeringen, *Phys. Rev.* **158**, 256 (1967); **181**, 125 (1969); W. van Haeringen and H. de Lang, *ibid.* **180**, 624 (1969); H. de Lang, D. Polder, and W. van Haeringen, *Philips Tech. Rev.* **32**, 190 (1971).
- [10] V. S. Smirnov and A. M. Tumaikin, *Opt. Spektrosk.* **33**, 107 (1972) [*Opt. Spectrosc.* **33**, 107 (1972)]; **36**, 546 (1974) [**36**, 315 (1974)]; **40**, 1030 (1976) [**40**, 593 (1976)].
- [11] D. Lenstra, *Phys. Rep.* **59**, 299 (1980).
- [12] W. R. Christian and L. Mandel, *Opt. Commun.* **64**, 537 (1987).
- [13] G. P. Puccioni, M. V. Tratnik, J. E. Sipe, and G. L. Oppo, *Opt. Lett.* **12**, 242 (1987).
- [14] C. Serrat, R. Vilaseca, and R. Corbalán, *Opt. Lett.* **20**, 1353 (1995); E. Roldán, G. J. de Valcárcel, R. Vilaseca, and R. Corbalán, *Phys. Rev. A* **49**, 1487 (1994); A. M. Kul'minskii, R. Vilaseca, and R. Corbalán, *Opt. Lett.* **20**, 2390 (1995).
- [15] W. Culshaw and J. Kannelaud, *Phys. Rev.* **141**, 228 (1966); J. Kannelaud and W. Culshaw, *ibid.* **141**, 237 (1966); W. Culshaw and J. Kannelaud, *ibid.* **156**, A308 (1967).
- [16] N. B. Abraham, E. Arimondo, and M. San Miguel, *Opt. Commun.* **117**, 344 (1995); see also **121**, 168 (E) (1995).
- [17] M. Matlin, R. S. Gioggia, N. B. Abraham, P. Glorieux, and T. Crawford, *Opt. Commun.* **119**, 204 (1995).
- [18] G. P. Puccioni, G. L. Lippi, N. B. Abraham, and F. T. Arecchi, *Opt. Commun.* **72**, 361 (1989).
- [19] M. A. van Eijkelenborg, C. A. Schrama, and J. P. Woerdman (unpublished); J. P. Woerdman, M. A. van Eijkelenborg, and M. P. van Exter, *Quantum Semiclassical Opt.* **7**, 591 (1995); M. A. van Eijkelenborg, C. A. Schrama, and J. P. Woerdman, *Opt. Commun.* **119**, 97 (1995).
- [20] U. Fano, *Rev. Mod. Phys.* **29**, 74 (1957); A. Omont, *J. Phys. (Paris)* **26**, 26 (1965); for an application in a different context, see also W. Happer and E. B. Saloman, *Phys. Rev. Lett.* **15**, 441 (1965).
- [21] M. I. D'Yakonov and V. I. Perel, *Zh. Eksp. Teor. Fiz.* **47**, 1483 (1964) [*Sov. Phys. JETP* **20**, 997 (1965)]; *Opt. Spektrosk.* **20**, 472 (1966) [*Opt. Spectrosc.* **20**, 257 (1966)].
- [22] See discussions by L. W. Casperson, in *Laser Physics*, edited by J. D. Harvey and D. F. Walls (Springer, Heidelberg, 1983), p. 88; *J. Opt. Soc. Am. B* **2**, 62 (1985); **2**, 77 (1985); **2**, 993 (1985); *Opt. Quantum Electron.* **18**, 274 (1986).
- [23] See the discussion by R. López-Ruiz, G. B. Mindlin, C. Pérez-García, and J. R. Tredicce, *Phys. Rev. A* **49**, 4916 (1994).
- [24] L. W. Hillman, J. Krasinski, R. W. Boyd, and C. R. Stroud, Jr., *Phys. Rev. Lett.* **52**, 1605 (1984); L. W. Hillman, J. Krasinski, K. Koch, and C. R. Stroud, Jr., *J. Opt. Soc. Am. B* **2**, 211 (1985); Fu Hong and H. Haken, *ibid.* **5**, 899 (1988).
- [25] V. M. Baev, J. Escher, E. Paeth, R. Schuler, and P. E. Toschek, *Appl. Phys. B* **55**, 463 (1992).
- [26] Ya. I. Khanin, *Principles of Laser Dynamics* (Elsevier, Amsterdam, 1995).
- [27] S. Grossman and D. Yao, *Z. Phys. B* **80**, 439 (1990); D. Yao and S. Grossman, *Z. Naturforsch. Teil A* **45**, 903 (1990).
- [28] C. A. Schrama, M. A. van Eijkelenborg, and J. P. Woerdman (private communication).
- [29] P. Chossat and M. Golubitsky, *Physica D* **32**, 423 (1988); I. Melbourne, in *Dynamics, Bifurcation and Symmetry, New Trends and Tools*, Vol. 437 of NATO Advanced Study Institute, Series B: Physics, edited by P. Chossat (Kluwer, Boston, 1994).
- [30] J. Redsnas, E. Roldán, and G. J. de Valcárcel, *Phys. Lett. A* **210**, 301 (1996); M. J. Tomás, E. Roldán, G. J. de Valcárcel, and R. Vilaseca, *Opt. Commun.* **114**, 111 (1995).